DYNAMIC ANALYSIS OF BRANCH SHAKING MACHINES VIA MULTI-DOF MODELING

Sezcan YILMAZ[1]

[1] Eskişehir Osmangazi University, Faculty of Engineering Architecture, Department of Mechanical Engineering, Eskişehir, Türkiye,
ORCID No: https://orcid.org/0000-0001-9329-5423

Keywords
Vibration–based harvesting
Branch shaking machines
Slider–crank mechanism
Multi-DOF modeling
Dynamic analysis

Abstract

In this study, the dynamic behavior of different types of branch shaking machines equipped with slider–crank mechanisms were investigated through a comparative approach. The systems were considered within a common kinematic framework and represented using a reduced single-axis model with three degrees of freedom along the dominant direction of motion. This modeling approach enabled a consistent comparison of different configurations while maintaining the essential dynamic characteristics of the system. Within this framework, the angular motion transmitted through the flexible shaft was converted into linear oscillatory motion via the slider–crank mechanism, and system interactions were represented using equivalent mass–spring–damper–friction elements. Different equipment configurations were evaluated based on whether the engine was externally mounted or integrated, as well as the positioning of the slider–crank mechanism relative to the operator or the branch. Simulation results were analyzed in terms of reaction forces transmitted to the user and displacement responses. The findings indicate that flexible shaft systems provide lower force transmission and improved user comfort, whereas configurations with the mechanism closer to the operator produce higher vibration amplitudes. Overall, the reduced modeling approach proved to be an effective tool for the rapid and comparative evaluation of alternative designs.

DAL SİLKELEME MAKİNELERİNİN ÇOK SERBESTLİK DERECELİ MODELLEME İLE DİNAMİK ANALİZİ

Anahtar Kelimeler
Titreşim tabanlı hasat
Dal silkeleme makineleri
Krank biyel mekanizması
Çok serbestlik dereceli modelleme
Dinamik analiz

Öz

Bu çalışmada, krank–biyel mekanizmasına sahip farklı tipteki dal silkeleme makinelerinin dinamik davranışları karşılaştırmalı bir yaklaşımla incelenmiştir. Sistemler, ortak bir kinematik çerçeve içinde ele alınmış ve baskın hareket doğrultusunda tek eksenli, üç serbestlik dereceli indirgenmiş bir model kullanılarak temsil edilmiştir. Bu modelleme yaklaşımı, sistemin temel dinamik özelliklerini korurken farklı konfigürasyonların tutarlı bir şekilde karşılaştırılmasına olanak sağlamıştır. Bu çerçevede, esnek şaft üzerinden iletilen açısal hareket krank–biyel mekanizması aracılığıyla doğrusal salınım hareketine dönüştürülmüş ve sistem etkileşimleri eşdeğer kütle–yay–sönüm–sürtünme elemanları ile ifade edilmiştir. Farklı ekipman konfigürasyonları, motorun harici veya tümleşik olması ile krank–biyel mekanizmasının operatöre ya da dala göre konumlandırılması açısından değerlendirilmiştir. Simülasyon sonuçları, kullanıcıya iletilen reaksiyon kuvvetleri ve yer değiştirme tepkileri temelinde analiz edilmiştir. Bulgular, esnek şaftlı sistemlerin daha düşük kuvvet iletimi sağlayarak kullanıcı konforunu artırdığını, buna karşılık mekanizmanın operatöre daha yakın konumlandırıldığı konfigürasyonların daha yüksek titreşim genlikleri ürettiğini göstermektedir. Genel olarak, indirgenmiş model yaklaşımının farklı tasarım alternatiflerinin hızlı ve karşılaştırmalı olarak değerlendirilmesi açısından etkili bir araç olduğu sonucuna varılmıştır.

Araştırma Makalesi		Research Article	
Başvuru Tarihi	: 22.04.2026	Submission Date	: 22.04.2026
Kabul Tarihi	: 11.06.2026	Accepted Date	: 11.06.2026

* Sorumlu yazar: sezcanyilmaz@ogu.edu.tr
https://doi.org/10.31796/ogummf.1936305

1. Introduction

The aim of mechanized harvesting in fruit trees is to overcome the maximum attachment force that keeps the fruit attached to the branch through various methods. In this approach, the objective is to increase the inertial forces generated by applying controlled vibrations to the trunk or branches, thereby producing dynamic loads that exceed the detachment threshold of the fruit. Achieving fruit detachment through this vibration-induced mechanism, while preserving the structural integrity of the tree, requires the proper selection of dynamic parameters such as amplitude, frequency, and acceleration (Pu, et al., 2023).

In vibration-based harvesting systems, excitation can be applied to the trunk, branches, or near the fruit at the branch tips (Farajijalal, Abedi, Manzo, Kouravand, Maharlooei, Toudeshki and Ehsani, 2025; Pu et al., 2023). In trunk-excited systems (Farajijalal et al., 2025; Láng, 2006; Cetinkaya, Polat and Ozalp, 2022), the entire tree mass is treated as a single dynamic system and forced vibrations with low-frequency–high-amplitude characteristics are typically generated. In this context, the tree can be modeled as a multi-degree-of-freedom system consisting of spring–mass–damper elements (Grande and Franceschini, 2024; Murphy and Rudnicki, 2012), and the applied vibrations result in energy transfer from the trunk to the branches (Deng et al., 2025; Liu, Kan, Yu, Zhou and Wang, 2026).

Trunk vibration systems can achieve high harvesting efficiency in a short time due to their ability to generate large dynamic loads. However, the large total mass of the system, the wide distribution of natural frequencies (Grande and Franceschini, 2024), and insufficient control of damping effects may lead to structural issues such as bark peeling, branch breakage, and damage in the root zone.

In branch vibration systems, excitation is applied locally to specific branches rather than to the entire tree (Dolma, Dixit Muzamil, Mushtaq, and Peerzada, 2024; Pu et al., 2023). In this approach, each branch is treated as an individual dynamic subsystem, and the branch–fruit interaction is typically represented using single- or two-degree-of-freedom vibration models. When the excitation frequency is selected close to the natural frequency of the branch, resonance effects increase the inertial forces acting on the fruit, enabling detachment with lower energy input. Although the harvesting rate in such systems is generally lower compared to trunk vibration methods, the dynamic loads transmitted to the overall tree structure are significantly reduced, thereby minimizing the risk of structural damage. Any potential damage is typically confined to the branch where the excitation is applied.

The effectiveness of different shaking methods varies depending on factors such as tree species, branch geometry, fruit mass, fruit–branch attachment stiffness, and system damping ratios (Pu et al., 2023). Therefore, determining an appropriate harvesting method requires identifying the dynamic characteristics of the tree through experimental (De Langre, 2019; Deng et al., 2025) or numerical approaches (De Langre, 2019; James, Dahle, Grabosky, Kane and Detter, 2014; Murphy and Rudnicki, 2012; Theckes, De Langre and Boutillon, 2011), and optimizing the vibration parameters accordingly (Kovacic, Zukovic and Radomirovic, 2018; Grande and Franceschini, 2024). In this context, modeling and analysis of vibration-based harvesting systems are of critical importance for both improving harvesting efficiency and preserving the long-term structural health of trees.

This study focuses on identifying the differences arising from the structural characteristics of various equipment commonly used to generate vibrations in tree branches through dynamic analysis. Within this scope, branch shaking equipment was first classified and examined based on their structural features, and subsequently, a kinematic model encompassing all configurations was developed. The model was simulated using the Simscape Foundation Library within MATLAB Simulink. The results obtained were then presented and comparatively evaluated.

2. Methods

In this study, research and publication ethics were compiled with.

2.1. Branch shaking equipment

Branch shaking equipment exhibits various configurations depending on their structural characteristics. However, an examination of commonly used systems shows that slider-crank mechanisms are predominantly preferred for vibration generation (Dolma et al., 2024). In such equipment, internal combustion engines are generally used as the primary power source. Nevertheless, with advancements in battery technologies, although not yet widespread, there are emerging applications where electric motors are employed as an alternative power source.

The equipment commonly used individually by operators for branch shaking operations has been classified in this study into four main groups, as presented in Figure 1. As can be seen from the figure, although all equipment share similar structural components, they differ in terms of component combinations and layout configurations.

In the equipment presented in Figure 1 (a) and (b), the slider-crank mechanism is positioned close to the branch. This configuration enables more direct transmission of vibration energy to the branch, thereby reducing transmission losses. The primary difference between these two configurations is that, in Figure 1 (a), the engine is located as an external unit and motion is transmitted to the crankshaft via a flexible shaft, whereas in Figure 1 (b), the engine is directly integrated into the equipment. The use of an external engine significantly reduces the mass of the handheld component, providing advantages in terms of operator ergonomics and prolonged use. However, the use of a flexible shaft introduces dynamic effects such as torsional flexibility, additional damping, and potential power losses. In contrast, the integrated engine design offers a more compact structure and more direct power transmission, although the increased mass may impose a greater load on the operator.

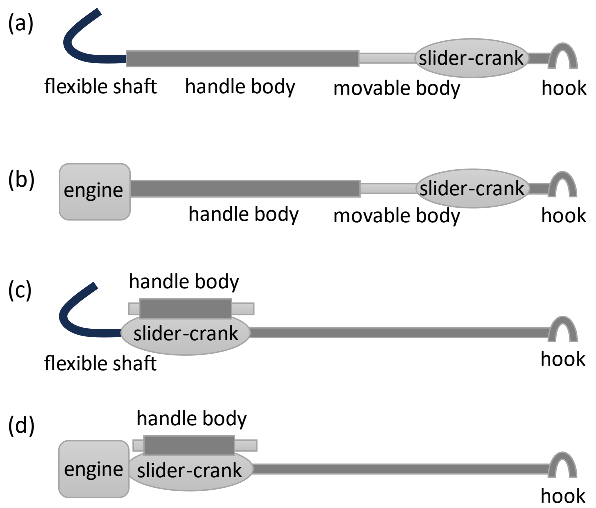

Figure 1. Branch Shaking Machines with the Slider-Crank Mechanism Located near the Branch: (a) Externally Powered and (b) Internally Powered Configurations; and with the Slider-Crank Mechanism Located near the Operator: (c) Externally Powered and (d) Internally Powered Configurations.

On the other hand, in the shaking equipment shown in Figure 1 (c) and (d), the slider-crank mechanisms are positioned closer to the operator. In such configurations, the reduced distance between the vibration source and the operator increases the potential for higher vibration transmission to the user. The main difference between these two systems again lies in whether the engine is configured as external or integrated. In externally powered systems, mass distribution and vibration transmission characteristics differ, whereas integrated engine systems provide a more compact and unified structure. The approximate technical specifications of commercially available branch shaking machines presented in Figure 1 are given in Table 1. The handle body mass and movable body mass were estimated approximately based on the total body mass of the equipment.

Table 1. Approximate Specifications of Commercially Available Branch Shaking Machines of Different Types.

Type	(a)	(b)	(c)	(d)
Handle body mass (kg)	2.0	9.5	1.0	1.0
Movable body mass (kg)	2.5	2.5	8.0	14.0
Hook mass (kg)	0.5	0.5	1.5	1.5
Rod stroke (mm)	40	40	50	50
Transmission ratio i	2.5	2.5	4.2	4.2
Max. crank speed (rpm)	4300	4300	2500	2400
Mean crank speed (rpm)	2500	2500	1500	1500

The parameters associated with the type (a) shaking equipment were determined based on the technical specifications of the commercially available Stella Plus SP-900 (body mass: 4.2 kg, rod stroke: 40 mm, vibrations per minute: 4300) and HFS-SA-0001 (body mass: 4.5 kg, rod stroke: 40 mm, vibrations per minute: 4300) models. These machines were selected as representative examples of branch-shaking systems in which the slider-crank mechanism is located near the branch and driven by an externally mounted engine through a flexible shaft.

For the type (b) shaking equipment, the HFS-YA-0008 model was used as the reference. This machine exhibits a structural configuration highly similar to that of the HFS-SA-0001. The primary distinction between the two designs is that, in the HFS-YA-0008, the engine is integrated directly into the handle body, increasing the overall body mass to approximately 12 kg.

The parameters corresponding to the type (d) shaking equipment were established using the technical specifications of the commercially available Cifarelli SC800 (body mass: 14.9 kg, rod stroke: 62 mm, vibrations per minute: >2000), STIHL SP 482 (body mass: 12.8 kg, hook mass: 1.3 kg, rod stroke: 45 mm, vibrations per minute: 3328), and Farmart BSA55PN-M (body mass: 15 kg, hook mass: 1.5 kg, rod stroke: 50 mm, vibrations per minute: 1850) models. These products were considered representative of branch-shaking machines in which the slider-crank mechanism is positioned close to the operator and the engine is integrated into the machine structure.

For the type (c) shaking equipment, the Farmart BSA63 (body mass: 8.75 kg, hook mass: 1.5 kg, rod stroke: 50 mm, vibrations per minute: 2500) model was selected as the reference. Structurally, this machine shares substantial similarities with the Farmart BSA55PN-M. The principal difference is that the engine is configured as an external unit rather than being integrated into the machine body, resulting in a lower mass of the handheld assembly.

The speed values reported for these machines are nominal values and represent the maximum speeds achievable depending on the engine and gearbox system used. However, under real operating conditions, the loads acting on the system cause deviations from these values. In particular, the interaction between parameters such as branch stiffness, damping characteristics, and mass, together with the maximum power provided by the engine, leads to a reduction in engine speed underload. The gearbox transmission ratio i is defined as the ratio of engine speed n_{engine} to vibration-unit crankshaft speed n_{crank}.

$$i = \frac{n_{engine}}{n_{crank}} \tag{1}$$

Two-stroke internal combustion engines, which are commonly used to drive such mechanisms, have maximum operating speeds of approximately 10000 rpm; however, under load, this speed can decrease to below 8000 rpm (Ausserer, Polanka, Baranski, Grinstead and Litke, 2017). In addition, it is reported in the literature that the centrifugal clutch mechanisms used in these engines engage at around 4,000 rpm. This defines the lower bound of the effective operating range of the engine. Accordingly, in practical applications, the stable operating speed range of these engines under load can be approximately 4,000–8,000 rpm.

Within the scope of this study, the engine was modeled as an ideal motion source with an average operating speed of 6,000 rpm under load for use in the dynamic analysis. This assumption was adopted both for consistency with typical operating ranges reported in the literature and to provide a representative operating point for the analysis.

2.2. Kinematic model

Despite differences in design and layout, branch shaking machines employing a slider-crank mechanism largely share a common kinematic structure. This enables different configurations to be analyzed within a comparable analytical framework. Figure 2 presents an idealized kinematic representation of a branch shaking operation based on a slider-crank mechanism.

Under real operating conditions, the system exhibits multi-degree-of-freedom behavior, involving both translational and rotational motions in three-dimensional space. However, considering the dominant dynamic characteristics of the system, it is assumed that performing a reduced analysis along the primary direction of motion provides sufficiently accurate results for understanding the overall system behavior. Accordingly, in the model presented in Figure 2, the angle θ_1 is assumed to be constant, while the motions of the engine crankshaft, handle body, movable body, and hook are treated as independent coordinates, resulting in a four-degree-of-freedom system. The motions of the handle body, movable body, and hook components are restricted to translational motion along the x-axis.

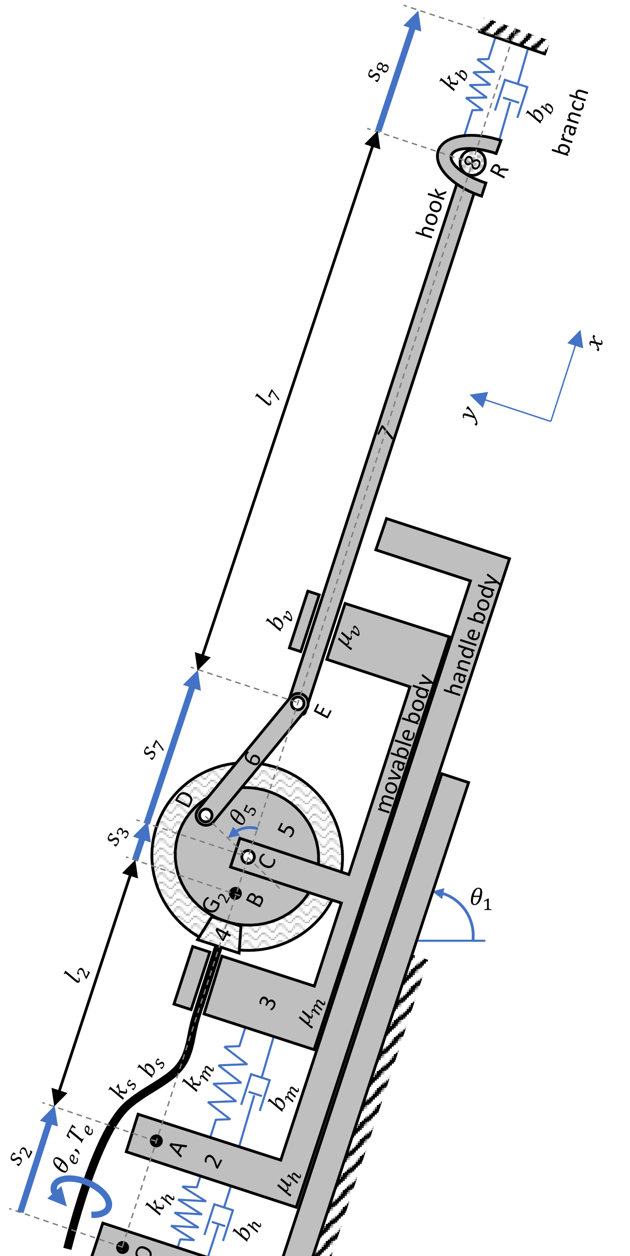

Figure 2. Branch Shaking Machines with the Slider-Crank Mechanism Located near the Branch: (a) Externally Powered and (b) Internally Powered Configurations; and with the Slider-Crank Mechanism Located near the Operator: (c) Externally Powered and (d) Internally Powered Configurations.

The angular motion of the engine crankshaft, denoted by θ_e, is transmitted to the pinion gear through the flexible shaft. The resulting pinion gear rotation θ_4, drives the crankshaft of the slider-crank mechanism mounted on the movable body. The kinematic relationship between the motion of the pinion gear θ_4, and the crankshaft rotation θ_5, is given by

$$\theta_5 = \frac{N_4}{N_5}\theta_4 \tag{2}$$

where N_4 and N_5 denote the numbers of teeth of the pinion gear and the crank gear, respectively.

The slider-crank mechanism, by its nature, is a single-degree-of-freedom mechanism that transmits input motion to the output through a defined kinematic relationship. In this context, the angular motion θ_5 of the crankshaft is transformed by the slider-crank mechanism into a periodic translational motion of the hook, represented by

$$s_7 = r_5 \cos\theta_5 + \sqrt{l_6^2 - r_5^2 \sin^2\theta_5} \tag{3}$$

where r_5 and l_6 denote the crank radius and the connecting rod length, respectively. Accordingly, the velocity of the slider can be expressed as

$$\dot{s}_7 = -\dot{\theta}_5 \sin\theta_5 \left(r_5 + \frac{r_5^2 \cos\theta_5}{\sqrt{l_6^2 - r_5^2 \sin^2\theta_5}} \right) \tag{4}$$

The slider velocity can be approximated as

$$\dot{s}_7 \approx -r_5 \dot{\theta}_5 \left(\sin\theta_5 + \frac{r_5}{2l_6} \sin 2\theta_5 \right) \tag{5}$$

Accordingly, the slider acceleration is given by

$$\ddot{s}_7 \approx -r_5 \dot{\theta}_5^2 \left(\cos\theta_5 + \frac{r_5}{l_6} \cos 2\theta_5 \right) \tag{6}$$

This transformation constitutes the fundamental mechanism of energy transfer between rotational and translational motion.

Among the displacement variables in the model, s_2 represents the absolute motion of the handle body relative to the operator, while s_3 denotes the relative motion of the movable body with respect to the handle body. These definitions enable the decomposition of dynamic interactions among intermediate masses within the kinematic chain. Elastic and damping effects in the system are represented using spring–damper–friction elements. The biomechanical effects of the operator are not modeled in detail (Yanikören, Yilmaz and Gündoğdu, 2024); instead, the operator–machine interaction is represented by an equivalent spring and damper. Accordingly, the parameters k_h, b_h, and μ_h denote the stiffness, viscous damping, and dry friction effects between the operator and the handle body, respectively, while k_m, b_m, and μ_m define the interactions between the handle body and the movable body. The damping and friction effects between the movable body and the hook are represented by b_v and μ_v. Finally, the mechanical properties of the branch, considered as an external load, are incorporated into the model through the parameters k_b and b_b, representing stiffness and damping, respectively. Although this reduced-order representation of the branch cannot fully capture its nonlinear and complex structural behavior, it is considered sufficiently accurate for comparative performance analysis of the equipment.

The reduced-order model developed in this manner (Kaya, Öztürk and Yılmaz, 2025; Öztürk and Yılmaz, 2026) provides a comprehensive representation that enables the analysis of the system's dynamic response, the investigation of parameter sensitivities, and the comparison of different design configurations.

2.3. Simulation

In the system presented in Figure 2, the connecting rod in the slider-crank mechanism exhibits planar motion with components in both the x and y directions. However, in this study, in order to reduce model complexity and focus on the dominant motion characteristics, a one-dimensional analysis approach is adopted by considering only the motion along the x-axis. Such a reduction significantly simplifies the analytical and numerical solution processes while preserving the essential dynamic features of the system.

The Simscape Foundation Library available in the MATLAB Simulink environment was used to simulate the kinematic structure shown in Figure 2 without deriving an analytical model (Das, 2021). The corresponding kinematic system was implemented in the Simulink environment using physics-based components, as shown in Figure 3. Examination of the model shows that the flexible shaft, which transmits the engine motion to the shaking mechanism, is represented by an equivalent combination of mass inertia, spring, and damping elements. This approach allows both torsional and axial flexibility effects of the shaft to be captured in a simplified manner. The motion obtained from the flexible shaft is transmitted to a gearbox, where it is adjusted to appropriate speed and torque levels before being delivered to the slider-crank mechanism. Within the slider-crank mechanism, rotational motion is converted into a periodic translational motion. However, since the slider-crank block available in Simulink is defined as an ideal mechanism, it does not directly account for flexibility and relative motion effects present in the real system. Therefore, instead of directly connecting the output of this block to link 7 (piston/hook), it is incorporated into the model as the velocity of the relative displacement s_7 between link 3 and link 7. This approach enables a more realistic representation of the system's dynamic behavior.

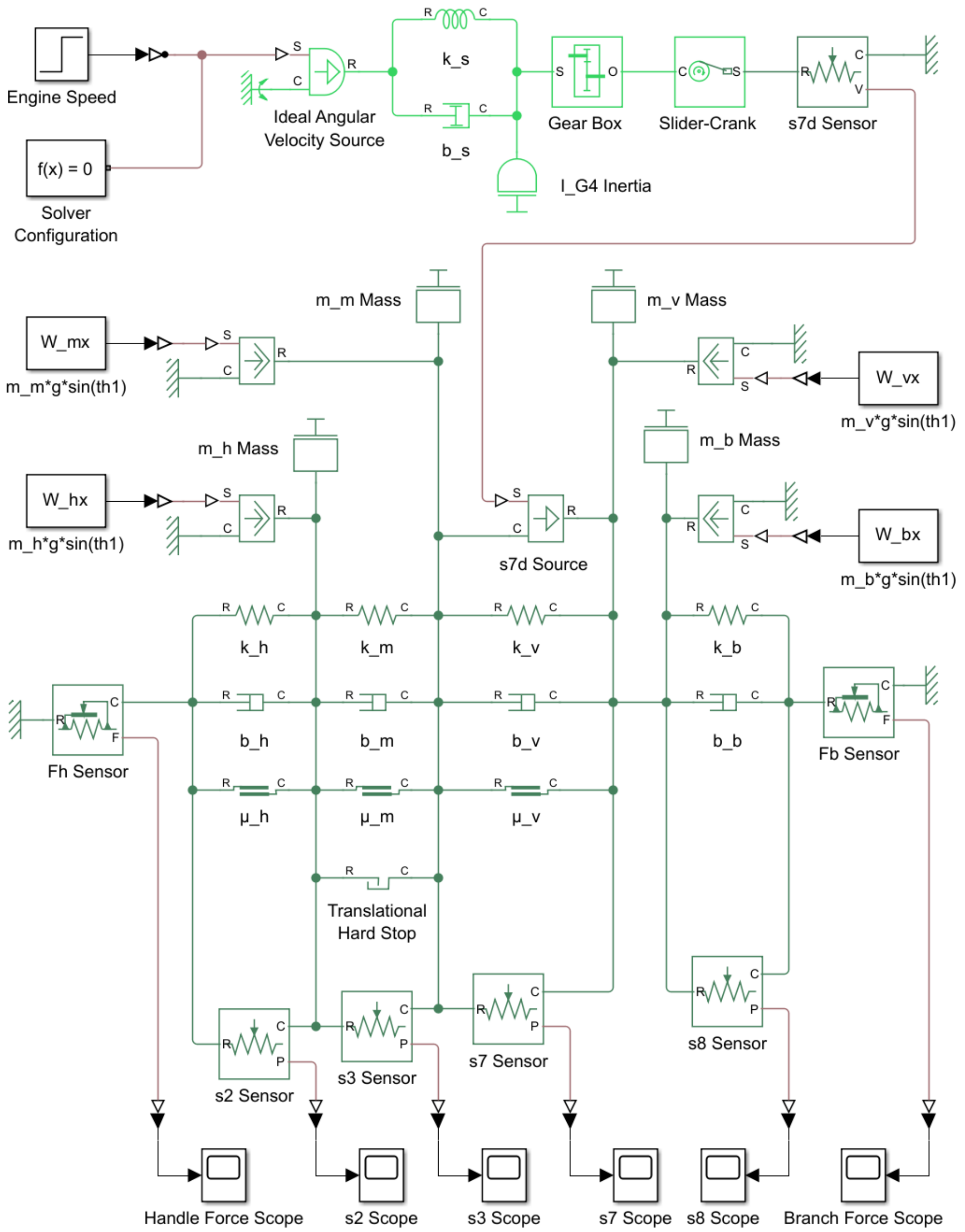

Figure 3. Simulink Model of the Branch Shaking Operation Using a Slider-Crank Mechanism.

The mass elements in the model are defined as m_h for the handle body, m_m for the movable body, m_v for the vibrating hook, and m_b for the branch. The mass-related parameters of the machines are presented in Table 1. The handle body mass represents the combined mass of the machine handle and the operator's arm. For the purposes of the simulations, the operator's arm mass was assumed to be 4 kg. Since the shaking machine operates at an angle θ_1 (or th1) relative to the horizontal plane, the projections of the gravitational forces acting on the moving components along the x-axis are also included in the model. Accordingly, W_{hx}, W_{mx}, W_{vx}, and W_{bx} represent the components of the gravitational effects of the respective masses in the direction of analysis.

In addition, the spring, damping, and friction elements used in the model are defined consistently with the kinematic representation presented in Figure 2. The parameter values of these elements used in the simulations are provided in Table 2.

Table 2. Parameters of the Spring and Damper Elements

Stiffness coefficient		Damping coefficient	
k_s	1 Nm/rad	b_s	0.01 Nm s/rad
k_h	300 N/m	b_h	20 Ns/m
k_m	2000 N/m	b_m	30 Ns/m
k_v	100 N/m	b_v	30 Ns/m
k_b	1500 N/m	b_b	15 Ns/m

The parameters of the flexible shaft stiffness k_s and damping b_s elements were approximately selected based on experimentally measured data reported in the literature (Usman et al., 2024).

In modeling the interaction between the operator and the handle body, the dominant mechanical characteristics are governed by the behavior of the operator's shoulder joint. The operator's muscular condition, grip force, and excitation frequency can cause the corresponding stiffness k_h and damping b_h coefficients to vary over a wide range, as reported in *ISO 10068:2012 Mechanical vibration and shock — Mechanical impedance of the human hand-arm system at the driving point*. Therefore, the $k_h$and b_h parameters were selected as approximate values under the assumption that the operator maintains a relatively loose grip intended primarily for alignment purposes rather than forceful restraint (Adewusi, Rakheja, and Marcotte, 2012; Dobry and Hermann, 2015).

The stiffness parameter k_m used to model the interaction between the handle body and the movable body was estimated from the geometric dimensions of the helical spring constituting the suspension system. In contrast, the damping parameter b_m represents the damping effect associated with the axial motion of the sliding bearing located between the handle body and the movable body and was assigned an approximate value in this study.

The stiffness k_v and damping b_v characteristics of the sliding bearing located between the movable body and the hook, together with the flexible rubber bellow used to protect the assembly from environmental conditions, exhibit significant variations depending on the excitation frequency (Chen et al., 2024). The stiffness value of the flexible rubber bellow, which has a thin-walled structure, was approximately determined through measurements performed on a representative sample. Assuming that the critical damping ratio of rubber materials varies between 0.05 and 0.15, the damping contribution of the rubber bellow was estimated to be approximately 1 Ns/m. However, when combined with the damping effects arising from the axial motion of the sliding bearing, the overall damping coefficient b_v was assumed to be approximately 30 Ns/m.

Studies on the damping characteristics of tree branches have shown substantial differences between measurements conducted during leafless and leafy periods (Sola-Guirado, Luque-Mohedano, Tombesi and Blanco-Roldan, 2022). Depending on the vibration mode and leaf density, the damping ratio may increase severalfold (Castro-Garcia, Blanco-Roldán, Gil-Ribes and Agüera-Vega, 2008). This increase in damping ratio consequently leads to an increase in the equivalent damping coefficient. Considering experimental investigations conducted on cherry trees (Grande and Franceschini, 2024) and olive trees (Sola-Guirado et al., 2022), it was concluded that for a leafy branch during the fruiting season, having a basal diameter of approximately 6 cm and tapering to about 4 cm at a distance of 1 m from the trunk, where the branch is grasped by the harvesting hook, representative values of $m_b = 5$ kg, $k_b = 1500$ N/m, and $b_b = 15$ Ns/m provide a reasonable approximation of the branch's equivalent dynamic properties.

For friction modeling, the breakaway and Coulomb friction coefficients for the shaft–bearing contacts represented by μ_m and μ_v were assumed to be 0.12 and 0.10, respectively (Beňo, Marienčík, Turis, Kozak and Konjatić, 2016). For the machine–operator interface, the breakaway and Coulomb friction coefficients μ_h were assumed to be 0.12 and 0.10, respectively. This selection is made to represent the different behaviors of dry friction during the initiation of motion and steady-state operation. Finally, the Translational Hard Stop element included in the model is used to define the physical limits of motion of the movable body relative to the handle body. This element represents the mechanical constraints present under real operating conditions, thereby contributing to the physical realism and applicability of simulation results.

The use of a step function as the motion input enables a more controlled establishment of the system's initial conditions. With this approach, the transient oscillations caused by gravitational effects associated with the angle θ_1 are allowed to decay before the shaft motion is activated. Consequently, the dynamic response of the system can be analyzed under steady operating conditions, free from initial transient effects. The step time parameter of the step function is selected by considering the initial behavior of the system under different configurations. Accordingly, for θ_1 values of 0°, 30°, and 60°, the step time is set to 2 s, 2.5 s, and 3 s, respectively. This selection accounts for the variation in gravitational force components and the corresponding increase in damping time with increasing inclination angle. Thus, for each angular condition, sufficient time is provided for the free vibrations to decay before the input is applied, ensuring consistent and comparable simulation results.

2.4. Limitations

The equivalent mass–spring–damper model employed to represent the branch cannot fully capture the nonlinear and complex structural behavior of a real branch, including its distributed mass and stiffness properties, higher-order vibration modes, and mode-dependent damping characteristics. Consequently, while the model is suitable for representing the dominant dynamic response of the branch and for comparing different branch-shaking machine configurations, it is not intended for detailed frequency-response analyses or comprehensive assessments of structural damage mechanisms. Nevertheless, it is considered an adequate approximation for investigating the fundamental dynamic characteristics of the shaking system.

In this study, the biomechanical effects of the operator were not modeled in detail. Instead, the operator–machine interaction was represented by an equivalent spring–damper element. While this simplification facilitates the solution of the model, it reflects the complex dynamics of human–machine interaction only to a limited extent.

Furthermore, the analyses were carried out under the assumption of single-axis motion (along the x-direction), and translational and rotational components in non-dominant axes were neglected. Therefore, the obtained results should be interpreted within the framework of the stated modeling assumptions and limitations; in particular, they should not be directly generalized to cases where multi-axis motion and nonlinear effects play a significant role.

In addition, the engine was represented as an ideal constant-speed source operating at 6000 rpm. As a result, load-dependent torque–speed variations of the engine were neglected, and the analyses were conducted under a steady-state kinematic boundary condition.

3. Results and Discussion

To evaluate the effects of equipment, use in different configurations on operator comfort, the reaction forces transmitted to the user through the handle component of the shaking machines presented in Figure 4 were comparatively examined together with the displacement responses given in Figure 5. Prior to the onset of the shaking operation, it was observed that the system exhibited transient oscillatory behavior under its own weight as the equipment was suspended from the branch.

When a general comparison is made, it is observed that the type (b) and type (d) shaking equipment results in both larger oscillation amplitudes and higher reaction forces transmitted to the user. In contrast, these effects are found to be more limited in configurations incorporating a flexible shaft. During the shaking operation, the minimum, maximum, and fluctuation range values of the reaction forces transmitted to the user through the handle are presented in Table 3. The fluctuation range of the reaction force is a more decisive criterion in terms of the vibration perceived by the user and the resulting level of discomfort. In this context, it is observed that the force fluctuation range is higher in type (c) and type (d) equipment, where the slider-crank mechanism is positioned closer to the user, leading to a negative effect on comfort. For the type (d) equipment with an integrated engine structure, the fluctuation of the reaction force is noticeably higher compared to the other configurations.

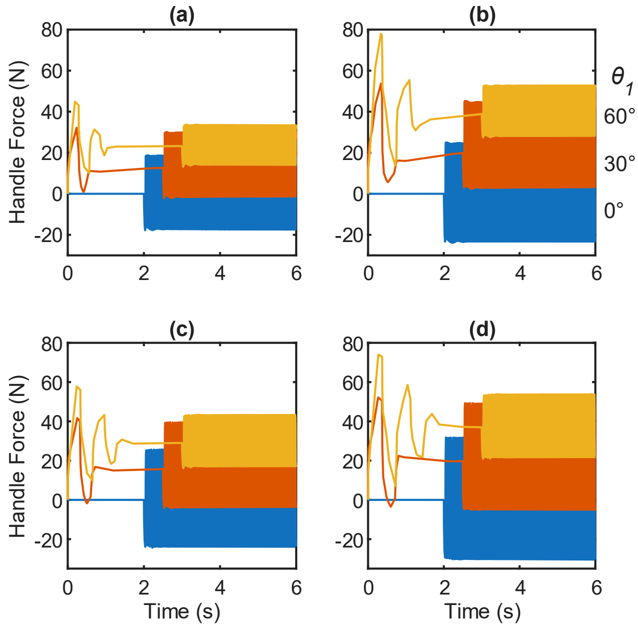

Figure 4. Reaction Forces Transmitted to the User through the Handle of Different Types of Branch-Shaking Machines at Various Operating Angles θ_1.

Table 3. Minimum, Maximum, and Range Values of the Reaction Forces Transmitted to the User through the Handle during the Shaking Operation.

Type	θ_1	Min. (N)	Max. (N)	Range (N)
(a)	0°	-17	18	35
	30°	-1	30	31
	60°	14	33	19
(b)	0°	-23	25	48
	30°	3	45	42
	60°	28	53	25
(c)	0°	-24	26	50
	30°	-4	40	44
	60°	17	43	26
(d)	0°	-30	31	61
	30°	-5	49	54
	60°	22	54	32

For all equipment types, it was determined that as the handle angle θ_1 increases, the maximum reaction force increases, whereas the fluctuation range of the force decreases significantly. This behavior can be interpreted as a relative suppression of dynamic fluctuations due to the increase in the static load components of the system.

Considering the principles outlined in ISO 5349 for the assessment of hand–arm vibration exposure, increased force fluctuations transmitted to the operator may be associated with higher vibration exposure levels and reduced user comfort. Although a quantitative evaluation in accordance with ISO 5349 is beyond the scope of the present study, the lower reaction force fluctuations observed in type (a) equipment suggest a potentially more favorable operating condition in terms of operator comfort.

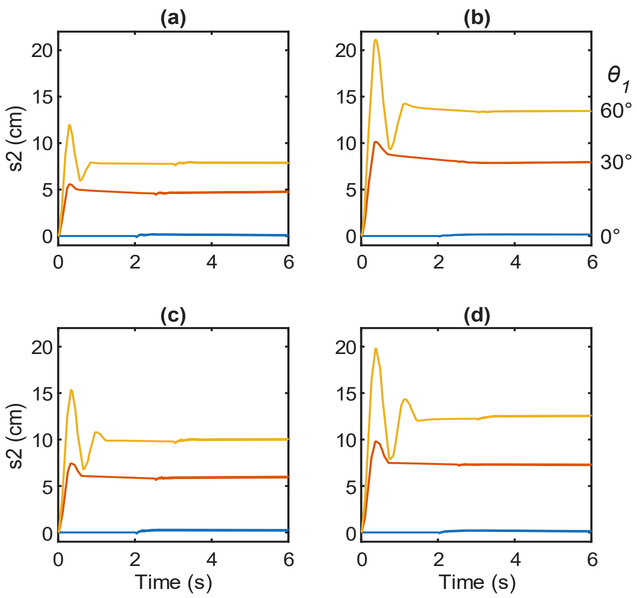

Figure 5. s_2 Displacements of Different Types of Branch-Shaking Machines during Operation at Various Operating Angles θ_1.

An examination of the results presented in Figure 6 indicates that the type (d) equipment generates significantly higher reaction forces on the branch compared to the other configurations. This force component does not directly contribute to the fruit detachment mechanism and essentially acts as a pulling force applied to the branch. Therefore, high levels of such forces are undesirable, as they may increase the risk of mechanical damage to the branch, and should be kept as low as possible.

The fluctuation range value of the reaction force presented in Table 4 can be considered a parameter directly related to fruit detachment from the branch. As the amplitude of the dynamic variation in the reaction force increases, the vibration energy transmitted to the branch also increases, contributing to a reduction in harvesting time. From this perspective, it is understood that equipment in which the slider-crank mechanism is positioned closer to the user generates higher force fluctuation ranges on the branch. The s_8 oscillation amplitude results presented in Figure 7 further support this finding. Higher displacement amplitudes indicate the generation of more effective vibrations on the branch and, consequently, an increase in fruit detachment efficiency.

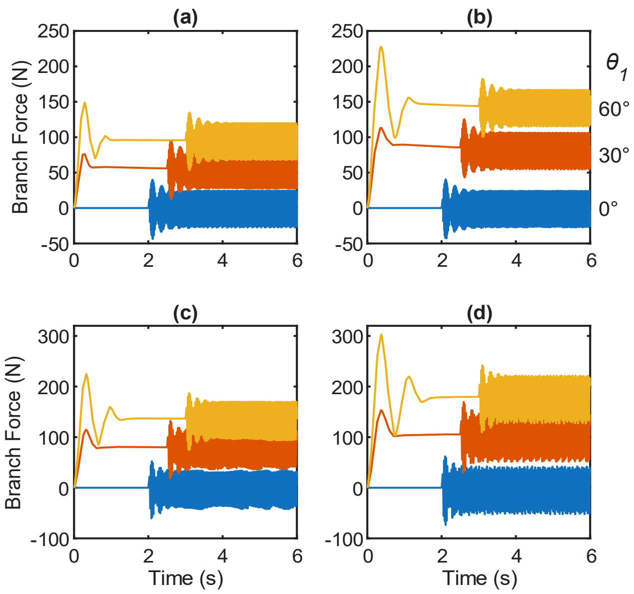

Figure 6. Reaction Forces Occurring between the Branch and the Trunk of the Tree for Different Types of Branch-Shaking Machines at Various Operating Angles θ_1.

Table 4. Minimum, Maximum, and Range Values of the Reaction Forces Occurring between the Branch and the Trunk during the Shaking Operation.

Type	θ_1	Min. (N)	Max. (N)	Range (N)
(a)	0°	-27	24	51
	30°	28	79	51
	60°	70	120	50
(b)	0°	-27	24	51
	30°	54	106	52
	60°	115	167	52
(c)	0°	-42	34	76
	30°	36	112	76
	60°	94	170	76
(d)	0°	-44	42	86
	30°	51	143	92
	60°	127	221	94

When a fast and efficient harvesting process is targeted, the type (d) equipment stands out as an advantageous option. However, considering the potential effects of increased force levels on branch damage, it is necessary to make a balanced choice between performance and structural integrity.

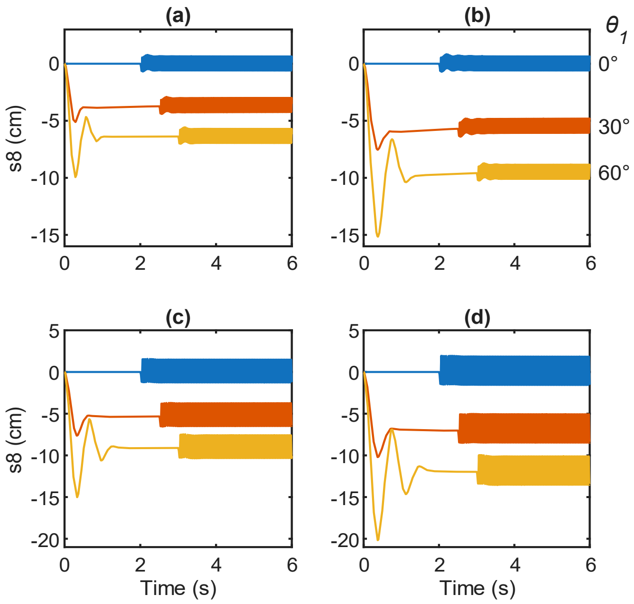

Figure 7. s_8 Displacement Responses of Different Branch-Shaking Machine Types at Various Handle Angles θ_1.

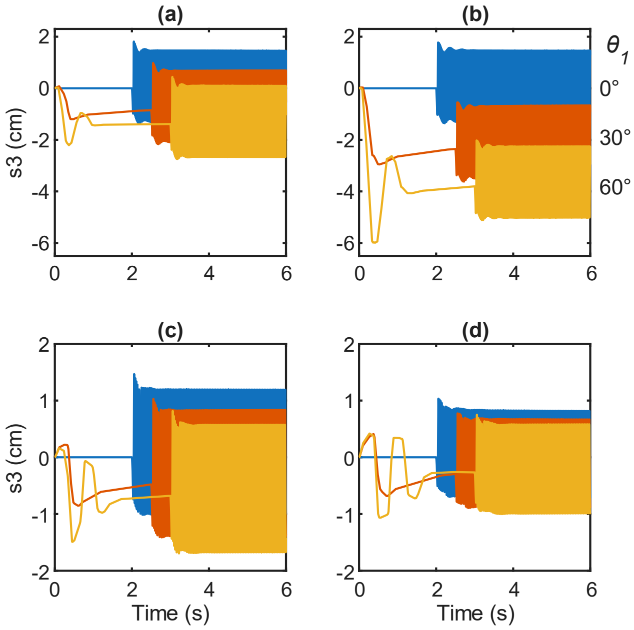

Figure 8. s_3 Displacement Responses of Different Branch-Shaking Machine Types at Various Handle Angles θ_1.

Figure 8 presents the s_3 motion, defined as the relative displacement of the movable body with respect to the handle body. Although this motion does not have a direct determining effect on user comfort or harvesting performance, it is desirable for it to remain as low as possible in terms of system integrity and mechanical stability. The simulation results indicate that, for all examined equipment configurations, the oscillation amplitude of the s_3 motion remains on the order of approximately 2 cm throughout the harvesting process. This value corresponds to an acceptable and well-controlled level of relative motion from a mechanical design perspective and indicates that no undesirable looseness or excessive deformation occurs within the system.

To provide additional insight into the frequency content of the branch force response, a Fast Fourier Transform (FFT) analysis was performed and the results are presented in Figure 9. The obtained spectra indicate that the dominant frequency components are concentrated around the excitation frequency and a low-frequency response component. Furthermore, the frequency spectra of type (a) and type (b) equipment exhibit nearly identical characteristics, while type (c) and type (d) equipment similarly show comparable spectral behavior within their own group.

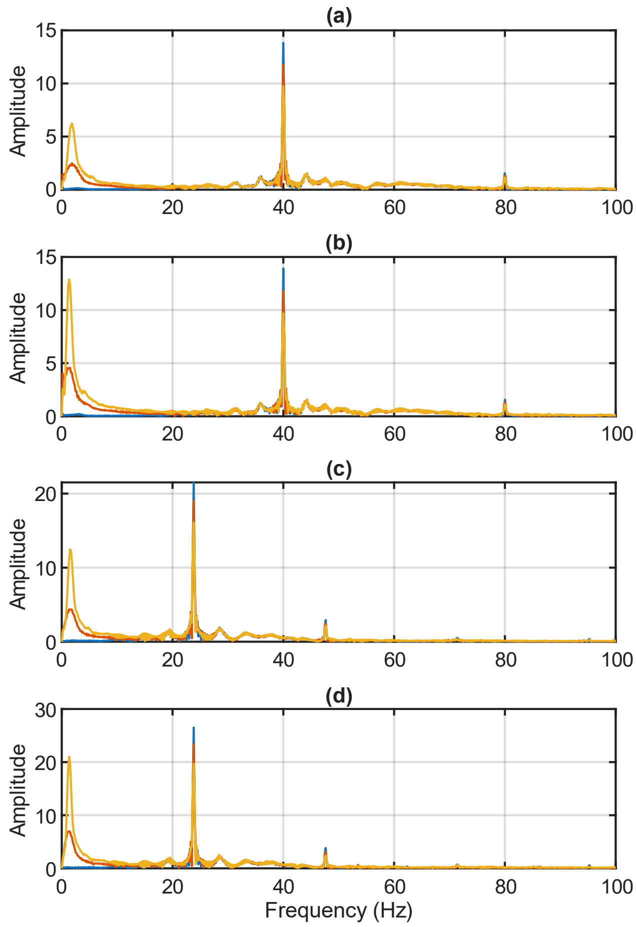

Figure 9. FFT Spectra of Branch Force Responses for the Investigated Branch-Shaking Machine Configurations.

It should be noted, however, that the branch was represented in the present study by an equivalent mass–spring–damper subsystem intended to capture the dominant dynamic behavior of the branch. Consequently, the model does not represent the distributed mass and stiffness characteristics of a real branch, nor its higher-order vibration modes. For this reason, any interpretation regarding potential structural damage mechanisms or resonance phenomena should be approached with caution. A more rigorous assessment of the relationship between excitation frequencies and branch structural integrity would require a higher-order branch model and, preferably, experimental validation under real operating conditions. Therefore, the FFT results presented herein should be considered primarily as a comparative indicator of the dynamic characteristics of the investigated machine configurations.

4. Conclusion

In this study, the dynamic behavior of branch-shaking machines with slider-crank mechanisms and different structural configurations was investigated through a reduced kinematic model and numerical simulations. It was demonstrated that the different designs share a common kinematic structure, and the system behavior was evaluated using a single-axis approach along the dominant direction of motion. This approach reduced model complexity while enabling the identification of the fundamental dynamic trends.

The findings reveal that design parameters in branch-shaking machines have a direct and significant influence on both performance and ergonomics. In particular, the location of the engine and the method of power transmission substantially affect both the vibration levels transmitted to the user and the dynamic impact on the branch. The results indicate a clear design trade-off between user comfort and harvesting efficiency, configurations that reduce vibration provide more comfortable operation, whereas systems that generate higher dynamic amplitudes enable faster harvesting. In addition, it should be considered that the high static force produced by certain configurations may increase the risk of branch damage.

In this context, an optimal design should be determined not only based on maximum performance but also by considering mechanical durability and operator ergonomics. In future studies, incorporating multi-axis motions, nonlinear branch behavior, and operator biomechanics into the model would contribute to obtaining more realistic and comprehensive results.

Acknowledgements

Artificial intelligence tools (ChatGPT) were used only for grammar correction and language editing in this manuscript.

Contribution of Researchers

In this study, conceptualization, writing, visualization, validation, simulation, methodology, formal analysis, and data curation were conducted by Sezcan YILMAZ.

Conflict of Interest

No conflict of interest was declared by the corresponding author.

References

Adewusi, S., Rakheja, S., & Marcotte, P. (2012). Biomechanical models of the human hand-arm to simulate distributed biodynamic responses for different postures. *International Journal of Industrial Ergonomics*, 42(2), 249-260. https://doi.org/10.1016/j.ergon.2012.01.005

Ausserer, J. K., Polanka, M. D., Baranski, J. A., Grinstead, K. D., & Litke, P. J. (2017). Measurement of loss pathways in small, two-stroke internal-combustion engines. SAE *International Journal of Engines*, 10(2), 128-143. https://doi.org/10.4271/2017-01-9276

Beňo, P., Marienčík, J., Turis, J., Kozak, D., & Konjatić, P. (2016). The friction factor dependence on the load and revolutions in sliding bearings without relubrication. *Tehnički vjesnik*, 23(4), 997-1001. https://doi.org/10.17559/TV-20140908114234

Castro-Garcia, S., Blanco-Roldán, G. L., Gil-Ribes, J. A., & Agüera-Vega, J. (2008). Dynamic analysis of olive trees in intensive orchards under forced vibration. *Trees*, 22(6), 795-802. https://doi.org/10.1007/s00468-008-0240-9

Cetinkaya, C., Polat, R., & Ozalp, A. F. (2022). Investigation of the vibration effect of using single or double eccentric mass in the trunk shakers used in fruit harvesting. *Engineering Science and Technology, an International Journal*, 35, 101228. https://doi.org/10.1016/j.jestch.2022.101228

Chen, Y., Qin, C., Zhou, H., Xu, Z., Xu, A., & Li, H. (2024). Damping characteristics of a novel bellows viscous damper. *Sensors,* 24(19), 6265. https://doi.org/10.3390/s24196265

Das, S. (2021). *Modeling for hybrid and electric vehicles using simscape*. Morgan & Claypool Publishers. https://doi.org/10.1007/978-3-031-01508-3_2

De Langre, E. (2019). Plant vibrations at all scales: a review. *Journal of Experimental Botany*, 70(14), 3521-3531. https://doi.org/10.1093/jxb/erz209

Deng, B., Wang, X., Wang, K., Song, H., Gao, S., Tu, Y., & Zhang, X. (2025). Analysis of energy transfer characteristics in multi-level branches of Lycium barbarum L. under vibration excitation. *Computers and Electronics in Agriculture*, 239, 110992. https://doi.org/10.1016/j.compag.2025.110992

Dobry, M. W., & Hermann, T. (2015). Differences in energy flow in three directions in Human-Tool biomechanical systems based on spatial human physical models specified in the ISO 10068: 2012 standard. *Journal of Theoretical and Applied Mechanics*, 53(4), 789-798. https://doi.org/10.15632/jtam-pl.53.4.789

Dolma, S., Dixit, J., Muzamil, M., Mushtaq, S. A., & Peerzada, H. A. (2024). Technical Feasibility and Economic Viability of Portable Limb Shaker in Apricot Harvesting at Union Territory of Ladakh, India. *Journal of Agricultural Engineering*, 61(4). https://doi.org/10.52151/jae2024614.1859

Farajijalal, M., Abedi, A., Manzo, C., Kouravand, A., Maharlooei, M., Toudeshki, A., & Ehsani, R. (2025). Assessing crucial shaking parameters in the mechanical harvesting of Nut trees: A review. *Horticulturae*, 11(4), 392. https://doi.org/10.3390/horticulturae11040392

Grande, E., & Franceschini, R. (2024). Calibration of mass-spring-damper equivalent systems for real time assessment of the dynamics of trees. *Computers and Electronics in Agriculture*, 227, 109610. https://doi.org/10.1016/j.compag.2024.109610

James, K. R., Dahle, G. A., Grabosky, J., Kane, B., & Detter, A. (2014). Tree biomechanics literature review: Dynamics. *Arboriculture & Urban Forestry (AUF)*, 40(1), 1-15. https://doi.org/10.48044/jauf.2014.001

Kaya, E., Öztürk, B., & Yılmaz, S. (2025). Development of scalable torque sensor for radial fans. *IEEE Sensors Journal*. https://doi.org/10.1109/JSEN.2025.3592855

Kovacic, I., Zukovic, M., & Radomirovic, D. (2018). Sympodial tree-like structures: from small to large-amplitude vibrations. *Bioinspiration & Biomimetics*, 13(2), 026002. https://doi.org/10.1088/1748-3190/aa9d1c

Láng, Z. (2006). Dynamic modelling structure of a fruit tree for inertial shaker system design. *Biosystems Engineering*, 93(1), 35-44. https://doi.org/10.1016/j.biosystemseng.2005.09.003

Liu, Y., Kan, J., Yu, C., Zhou, Y., & Wang, K. (2026). Branch-adaptive MDOF dynamic simulation modelling for vibration harvesting in Prunus cerasifera: An integrated computational and experimental analysis. *Biosystems Engineering*, 265, 104444. https://doi.org/10.1016/j.biosystemseng.2026.104444

Murphy, K. D., & Rudnicki, M. (2012). A physics-based link model for tree vibrations. *American Journal of Botany*, 99(12), 1918-1929. https://doi.org/10.3732/ajb.1200141

Öztürk, B., & Yılmaz, S. (2026). Dynamic modeling and analysis of a battery-powered screwdriver equipped with a hammer mechanism. *Mechatronics*, 116, 103483. https://doi.org/10.1016/j.mechatronics.2026.103483

Pu, Y., Wang, S., Yang, F., Ehsani, R., Zhao, L., Li, C., Xie, S., & Yang, M. (2023). Recent progress and future prospects for mechanized harvesting of fruit crops with shaking systems. *International Journal of Agricultural and Biological Engineering*, 16(1), 1-13. https://doi.org/10.25165/j.ijabe.20231601.7954

Sola-Guirado, R. R., Luque-Mohedano, R., Tombesi, S., & Blanco-Roldan, G. (2022). Effect of leaves in the dynamic response of olive tree branches and their computational model. *Computers and Electronics in Agriculture*, 203, 107490. https://doi.org/10.1016/j.compag.2022.107490

Theckes, B., De Langre, E., & Boutillon, X. (2011). Damping by branching: a bioinspiration from trees. *Bioinspiration & biomimetics*, 6(4), 046010. https://doi.org/10.1088/1748-3182/6/4/046010

Usman, M., Khorasani, A., Hubert, T., Furnémont, R., Vanderborght, B., Lefeber, D., Van de Perre, G. & Verstraten, T. (2024). Modeling of flexible shaft for robotics applications. *Mechanism and Machine Theory*, 197, 105647. https://doi.org/10.1016/j.mechmachtheory.2024.105647

Yaniküren, M., Yilmaz, S., & Gündoğdu, Ö. (2024). 3D biomechanical model that can perform dynamic analysis of the upper extremity and L5/S1 joints without the use of force sensor. *Sādhanā*, 49(3), 241. https://doi.org/10.1007/s12046-024-02590-0